AGU PUBLICATIONS

Geophysical Research Letters

RESEARCH LETTER
10.1002/2015GL067137

Key Points:
- Isoprene increases even with CO_2 inhibition effect
- Climate is the major driver for SOA increase
- Reduced anthropogenic emissions decreases SOA

Supporting Information:
- Supporting Information S1

Correspondence to:
G. Lin,
gxlin@umich.edu

Citation:
Lin, G., J. E. Penner, and C. Zhou (2016), How will SOA change in the future?, *Geophys. Res. Lett.*, *43*, 1718–1726, doi:10.1002/2015GL067137.

Received 23 NOV 2015
Accepted 21 JAN 2016
Accepted article online 28 JAN 2016
Published online 17 FEB 2016

How will SOA change in the future?

Guangxing Lin[1,2], Joyce E. Penner[1], and Cheng Zhou[1]

[1]Department of Atmospheric, Oceanic, and Space Sciences, University of Michigan, Ann Arbor, Michigan, USA, [2]Now at Atmospheric Sciences and Global Change Division, Pacific Northwest National Laboratory, Richland, Washington, USA

Abstract Secondary organic aerosol (SOA) plays a significant role in the Earth system by altering its radiative balance. Here we use an Earth system model coupled with an explicit SOA formation module to estimate the response of SOA concentrations to changes in climate, anthropogenic emissions, and human land use in the future. We find that climate change is the major driver for SOA change under the representative concentration pathways for the 8.5 future scenario. Climate change increases isoprene emission rate by 18% with the effect of temperature increases outweighing that of the CO_2 inhibition effect. Annual mean global SOA mass is increased by 25% as a result of climate change. However, anthropogenic emissions and land use change decrease SOA. The net effect is that future global SOA burden in 2100 is nearly the same as that of the present day. The SOA concentrations over the Northern Hemisphere are predicted to decline in the future due to the control of sulfur emissions.

1. Introduction

Secondary organic aerosol (SOA) has been shown to be an important component of nonrefractory submicron aerosol in the atmosphere [*Jimenez et al*., 2009]. The presence of SOA can influence the Earth's radiative balance by contributing to the absorption and scattering of radiation (the direct effect) and by altering the properties of clouds (indirect effects) [*Intergovernmental Panel on Climate Change* (*IPCC*), 2013].

A large fraction of total SOA originates from biogenic volatile organic compounds (BVOCs) [*IPCC*, 2013; *Lin et al*., 2012, 2014], emissions of which depend on temperature, nutrient availability, soil moisture, foliar biomass, leaf age, atmospheric composition, vegetation type, and species composition [*Guenther et al*., 2006]. Rising future temperatures could lead to increased BVOC emissions and SOA concentrations in the atmosphere, which in turn could moderate the warming via the aerosol direct and indirect effect [*Kulmala et al*., 2004].

However, this BVOC-SOA-climate interaction can be more complex than originally thought. The future increase in CO_2 concentration may directly inhibit isoprene (one major BVOC) emissions [*Arneth et al*., 2007], while CO_2 fertilization would enhance the emission rate through increasing photosynthesis [*Unger*, 2013]. Land use and land cover change caused by human activities have also been shown to be a major driver of global isoprene emission change for future climate [*Tai et al*., 2013]. Natural vegetation redistribution due to climate change could be a dominant control on isoprene emissions as well [*Lathiere et al*., 2005]. Additionally, the SOA concentration in the atmosphere not only depends on BVOC emissions but also is controlled by anthropogenic emissions, temperature, precipitation, and the oxidative capacity of the atmosphere [*IPCC*, 2013]. Exploring these complex interactions is quite challenging. It requires an Earth system model, fully coupling a BVOC emission model that represents these BVOC emission drivers, together with a sophisticated atmospheric model of SOA formation and properties.

Global chemistry-climate models predict an increase in isoprene emissions of 22–55% by 2100 due to the climate effect alone [*Liao et al*., 2006; *Heald et al*., 2008] and a change in the global SOA mass burden of 26% to 150% through the BVOC emission change and the climate-induced changes in aerosol formation and removal rates [*Liao et al*., 2006; *Tsigaridis and Kanakidou*, 2007; *Heald et al*., 2008]. However, none of the above studies account for the potential impact of direct CO_2 inhibition on BVOC emissions. In addition, all of the above estimates were made using simplified chemical mechanisms that are tuned to fit smog chamber data, do not follow the full time evolution of VOC oxidation to form SOA, and thus cannot account for the full complexity and the dynamics of the real SOA system [*Lin et al*., 2012, 2014]. Moreover, all of previous studies are limited to the SOA formed from the gas-particle partitioning, neglecting the SOA formed from heterogeneous chemical reactions in cloud or aerosol water. Yet the SOA formed from

the uptake of glyoxal, methylglyoxal, and isoprene epoxydiols (IEPOX) has been shown to contribute a nonnegligible fraction to ambient OA [*Ervens et al*., 2011; *Hu et al*., 2015]. Although many models have focused on the effect of primary organic aerosol (POA) and NO_x on SOA concentrations [*Tsigaridis and Kanakidou*, 2007; *Lane et al*., 2008; *Hoyle et al*., 2009; *Carlton et al*., 2010], no model has focused on the impact of sulfate and its associated water on SOA, although this has been observed in ambient data [*Xu et al*., 2015; *Nguyen et al*., 2015]. All of these call into the question of the validity and completeness of previous SOA projections.

This paper is based on previous studies of BVOC-chemistry-climate interactions and recent progress in SOA modeling and estimates future SOA using an Earth system model. The goal of this paper is (1) to quantify the change in SOA concentrations in response to climate and anthropogenic emissions change, and human land use change and (2) to assess the relative role of individual drivers on SOA change.

2. Model Description

To simulate the present-day climate, we employ Community Earth System Model (CESM) version 1.2.2 with the F_2000_CAM5 component set, which uses the global National Center for Atmospheric Research (NCAR) Community Atmospheric Model version 5.3 (CAM5.3) (http://www.cesm.ucar.edu/models/cesm1.2/cam/) and the NCAR Community Land Model version 4 (CLM4) [*Lawrence et al*., 2011] but prescribes sea surface temperature and sea ice fractions. We use the University of Michigan IMPACT aerosol model, which is embedded into CAM5.3 as a module, to simulate SOA concentrations. While CAM5.3 provides the necessary meteorology to the IMPACT aerosol module at each time step, changes to the aerosols in IMPACT do not provide feedback to CAM5.3. The IMPACT aerosol module simulates a total of six externally mixed aerosol types: pure sulfate aerosol, fossil fuel/biofuel primary organic aerosol (POA) and black carbon (BC), biomass burning POA and BC, SOA, sea salt, and dust. All the nonsulfate aerosols are internally mixed with sulfate through condensation and coagulation processes or through sulfate formation in cloud drops. The IMPACT aerosol module without the SOA component is described in *Zhou and Penner* [2014]. Here we also incorporate an explicit SOA formation scheme into the IMPACT aerosol module. The detailed description for this scheme is described in *Lin et al*. [2012] and *Lin et al*. [2014]. Briefly, in this explicit scheme, a detailed gas phase mechanism [*Ito et al*., 2007; *Lin et al*., 2012] is used to predict the formation of semivolatile organic products, which mainly consist of organic nitrates and peroxides from the oxidation of isoprene, α-pinene, and aromatics. These semivolatile organics partition into existing organic aerosols using the theory developed by *Pankow* [1994], with an explicit calculation of partitioning coefficients for each semivolatile compound. Lower volatility compounds (i.e., oligomers) are formed from these compounds after partitioning to the aerosol phase using an assumed formation time constant (nominally 1 day *e*-folding lifetime, though other time constants have been tested [*Lin et al*., 2012]). In addition to the SOA from the traditional gas-particle partitioning, SOA formation from aqueous phase reactions of glyoxal and methylglyoxal and from heterogeneous reactions of IEPOX is also included. Glyoxal and methylglyoxal partition into the cloud droplets (assuming Henry's Law) and undergo reactions to form organic acids [*Lin et al*., 2014]. Glyoxal, methylglyoxal, and IEPOX form low-volatility products on immediate kinetic uptake by sulfate-containing aerosols [*Lin et al*., 2012, 2014].

The anthropogenic and biomass burning emissions (both gas species and aerosol species) are adopted from those used in Community Atmosphere Model with Chemistry [*Lamarque et al*., 2012] for present-day (year 2000) simulations and from representative concentration pathways (RCP) for the 8.5 scenario [*van Vuuren et al*., 2011] for future (year 2100) simulations. RCP 8.5 emissions would give us the potential maximum climate and human activity effects on SOA concentrations. Biogenic VOC species are predicted from MEGAN 2.1 (Model of Emissions of Gases and Aerosols from Nature, version 2.1) [*Guenther et al*., 2012] embedded in CLM4. In MEGAN 2.1, canopy-level emission fluxes of each terrestrial BVOC are estimated as functions of light, temperature, leaf area index, and CO_2 inhibition. Annual mean global emissions for each species are listed in Table S1 in the supporting information. Removal of species occurs through dry deposition and wet deposition. Dry deposition follows a resistance-in-series parameterization [*Wesely*, 1989]. Gravitational setting is also taken into account for aerosol species [*Seinfeld and Pandis*, 1998]. Wet deposition is calculated using the scavenging module developed by *Mari et al*. [2000] and *Liu et al*. [2001], which includes scavenging in convective updrafts and first-order rainout and washout in precipitating columns.

Table 1. Estimates of Global Isoprene Emission, SOA Production Rate, Burden, and Lifetime for Seven Simulations

Simulation	CL2000_ EM2000[a]	CL2000_ EM2100[a]	CL2100_ EM2000[a]	CL2100_ EM2100[a]	CL2100_ EM2100_LND[a]	CL2000_ EM2000_pH[a]	CL2000_ EM2100_pH[a]
Isoprene emission (Tg/yr)	440	440	534	534	482	440	440
SOA production rate (Tg/yr)	55.4	48.7	65.4	55.3	48.4	55.7	47.4
SOA burden (Tg)	1.06	1.04	1.33	1.23	1.08	1.07	1.01
Lifetime (days)	7.00	7.83	7.40	8.13	8.11	7.00	7.81

[a]CL stands for climate; EM stands for anthropogenic emission; CL2000_EM2000 uses the year 2000 climate and anthropogenic emission; CL2000_EM2100 uses the year 2000 climate and the year 2100 anthropogenic emission; CL2100_EM2000 uses the year 2100 climate and the year 2000 anthropogenic emission; and CL2100_EM2100 uses the year 2100 climate and the year 2100 anthropogenic emission. CL2100_EM2100_LND is the same as CL2100_EM2100 but uses the year 2100 land cover. CL2000_EM2000_pH is the same as CL2000_EM2000 but takes into account the aerosol acidity effect on IEPOX uptake; CL2000_EM2100_pH is the same as CL21000_EM2100 but takes into account the aerosol acidity effect on IEPOX uptake.

3. Simulation Setup

Five simulations are designed to estimate the SOA levels in the present day (year 2000) and future (year 2100) to identify the relative role of climate change, anthropogenic emissions change, and anthropogenic land use change on SOA change (Table 1). CL2000_EM2000 simulation is performed with present-day climate and anthropogenic emissions, while CL2100_EM2100 simulation is run with future climate and anthropogenic emissions. For future year 2100 climate simulations, we apply monthly mean time-varying sea surface temperatures and sea ice distributions generated by the CESM 1.1.1 using the RCP 8.5 emissions [*Perket et al*., 2014; *Meehl et al*., 2013]. CL2000_EM2100 simulation keeps present-day climate but uses year 2100 anthropogenic emissions; CL2100_EM2000 simulation utilizes year 2100 climate and present-day anthropogenic emissions. In all but CL2100_EM2100_LND simulations, we apply fixed vegetation with present-day Moderate Resolution Imaging Spectroradiometer satellite-derived leaf area indices (LAIs) and fractional coverage of plant function types (PFTs). The CL2100_EM2100_LND simulation is the same as CL2100_EM2100 but with future PFT distributions, which take into account the anthropogenic land use/land cover change under the RCP8.5 scenario [*Lawrence et al*., 2012]. Changes in climate-sensitive natural emissions (e.g., isoprene) occur as a result of climate change and also respond to changes in CO_2 concentrations (which are included in the climate change scenario). Each model simulation is performed for 5 years with a 1 year spin-up. Results are averaged for the last 4 years.

The reactive uptake of IEPOX onto particles has been shown to be more efficient at higher particle acidities [*Eddingsaas et al*., 2010; *Piletic et al*., 2013; *Gaston et al*., 2014; *Riedel et al*., 2015]. Therefore, we conducted two sensitivity simulations (CL2000_EM2000_pH and CL2000_EM2100_pH) to examine the effect of aerosol acidity on the present-day and future SOA concentrations. The setup of CL2000_EM2000_pH and CL2000_EM2100_pH is the same as that for CL2000_EM2000 and CL2000_EM2100, respectively, except that the former two simulations take the aerosol acidity into account in the reactive uptake of IEPOX. The treatment for uptake, including the aerosol acidity dependence, follows *Pye et al*. [2013] and is described in detail in the supporting information.

4. Results

The present-day simulation (CL2000_EM2000) estimates a 55.4 Tg/yr global SOA production rate and 1.06 Tg SOA burden. About 80.5% of SOA in the present day is produced from the oxidation of isoprene, 8.5% is from monoterpene, and 11% from anthropogenic emissions. The largest SOA concentrations exist in tropical regions over South America and Africa because of these regions' large isoprene emissions and POA emissions (Figures 1a and 1b). There are also secondary maximum SOA concentrations in North America, Europe, and South East Asia, generally reflecting local anthropogenic emissions (Figures 1a and 1b). Compared to surface Aerosol Mass Spectrometer measurements reported in the literature (see Figure S1), the modeled present-day SOA concentrations are lower than measurements by 57% in the Northern Hemisphere and higher by 41% in the tropical forest regions. This is within the range of model-observation comparisons shown in *Tsigaridis et al*. [2014] for the AeroCOM organic aerosol model intercomparison project.

When the aerosol acidity effect is considered in the uptake of IEPOX in simulation CL2000_EM2000_pH, the global average SOA burden and production rate change very little (by 0.5%; Table 1). The burden of SOA

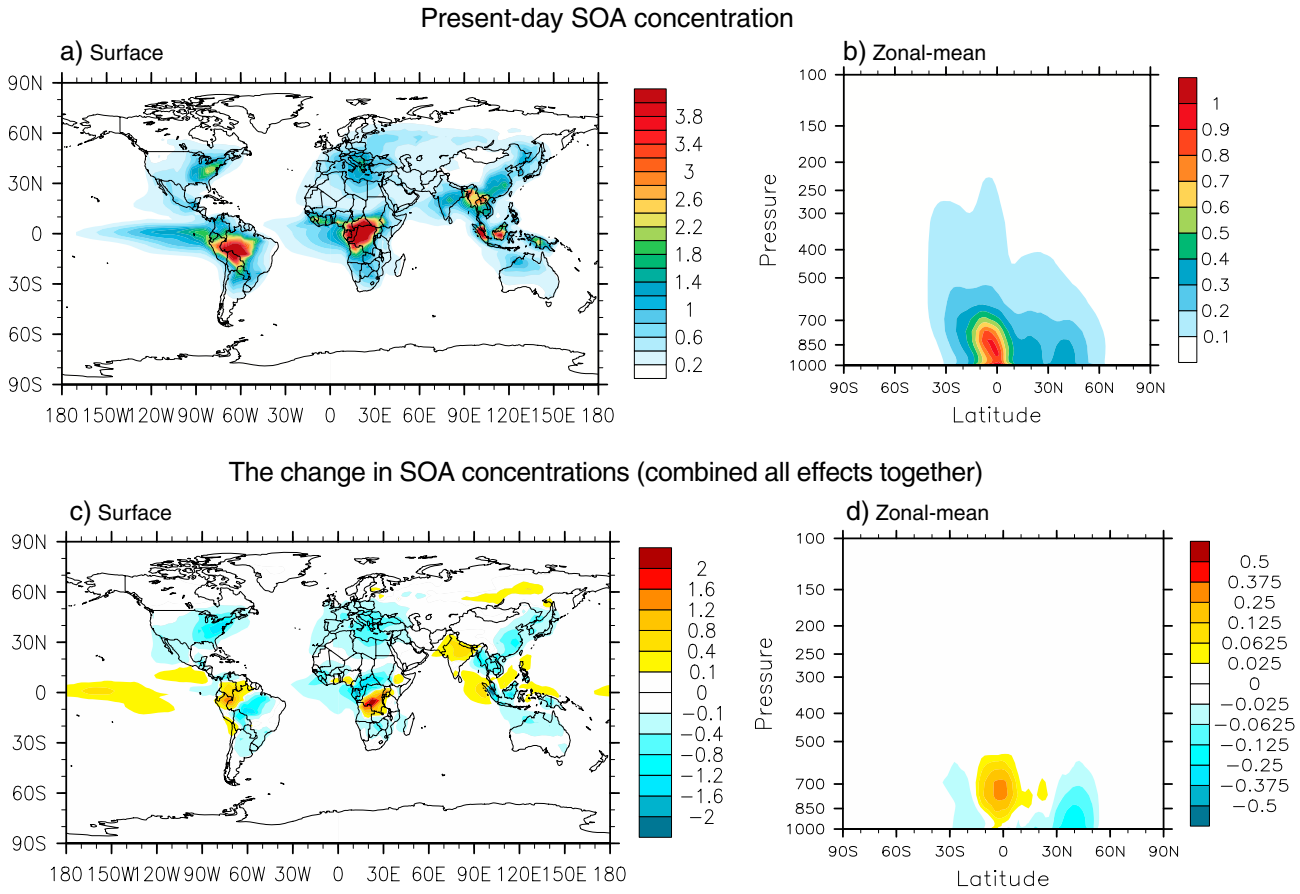

Figure 1. (a) Estimated year 2000 surface SOA concentrations and (b) zonally averaged vertical SOA concentrations. Projected year 2000 to year 2100 change in (c) surface SOA concentrations and (d) vertical SOA concentrations in response to the integrated effects of changes to anthropogenic emissions, climate, and anthropogenic land use change (CL2100_EM2100_LND-CL2000_EM2000). All units are in $\mu g/m^3$.

formed from the uptake of IEPOX from the surface to 900 hPa is decreased by 2%, while the burden above 900 hPa is enhanced by 2.5% (Figure S2). The reduction in the lower atmosphere is due to smaller reactive uptake coefficients, resulting in less uptake of gas phase IEPOX on aerosols. This allows more gas phase IEPOX to transport to the upper tropical atmosphere through the strong convection, producing more IEPOX SOA at higher altitudes. The comparisons of SOA with measurements are almost the same as those for the simulation with a constant IEPOX reactive uptake coefficient (Figure S1).

4.1. Effect of Anthropogenic Emission Change

In CL2000_EM2100 simulation, the global annual mean production rate of SOA formed from gas-particle partitioning decreases by 3%, due to the combined effect of decreases in POA emission and NO_x emissions and increases in aromatic emissions. Global POA emissions are projected to fall by 33% in the RCP 8.5 scenario. This decrease reduces the condensation mass on which semivolatile organic compounds condense. Aromatic emissions are predicted to increase by 31%, which increases the anthropogenic source for SOA from gas-particle partitioning by 20%. Global NO_x emissions are projected to decline by 10% in year 2100, which favors the reactions of organic peroxy radicals (RO_2) with HO_2 compared to those of RO_2 with NO. This would increase the formation of organic hydroperoxides, one major type of semivolatile organic compound predicted in the model, which contributes to a 20% increase in the global burden of gaseous semivolatile organic compounds. Hydroxyl radical burden in the troposphere decreases by 23%, largely as a result of the increase in CH_4 concentrations. The lower hydroxyl radical concentration slows the oxidation of hydrocarbons and delays subsequent SOA formation, thus forming longer-lived SOA aloft. Consequently, the global burden of SOA formed from gas-particle partitioning slightly increases (by 10%) in year 2100, despite the 2% decline in the SOA production rate.

The burden of SOA formed from the uptake of glyoxal, methylglyoxal, and IEPOX on sulfate aerosol is estimated to decrease by 43%, 54%, and 14%, respectively. The major reason for these decreases is the reduction of sulfate aerosol concentrations resulting from the control of sulfur emissions. The global sulfate burden decreases by 46% in year 2100. This reduces the total aerosol water content that can take up glyoxal, methylglyoxal, and IEPOX to form SOA. The global burdens of gas phase glyoxal, methylglyoxal, and IEPOX increase by 10%, 4%, and 25%, which is expected to increase their corresponding SOA concentrations. However, this increase is minor compared to the effect of decreased sulfate concentrations, causing the concentration of SOA formed from the uptake of glyoxal, methylglyoxal, and IEPOX on sulfate aerosol to decrease. The global burden of SOA formed in cloud water increases by 15%, as a result of the increase of gas phase glyoxal and methylglyoxal concentrations.

Overall, the change in anthropogenic emissions induced by 2100 RCP 8.5 scenario decreases the global SOA burden by 2% (Table 1) assuming no change in the present-day climate and land use (CL2000_EM2100-CL2000_EM2000). The small decrease in global SOA results from the net effect of the increase in SOA from gas-particle partitioning (+0.06 Tg or +10%), the decrease in SOA from the uptake of glyoxal, methylglyoxal, and IEPOX on sulfate aerosols (−0.1 Tg or −24%), and the increase in SOA from the uptake of glyoxal and methylglyoxal in cloud (+0.02 Tg or +43%).

The surface distribution of the change in total SOA resulting from the change in emissions is shown in Figure S3a, and the vertical distribution is shown in Figure S3b. Apparently, the SOA concentration at the surface decreases over most regions, except for India and Africa excluding Central Africa, where POA emissions are projected to increase. The largest decrease occurs over eastern U.S., Europe, and eastern China due to the significant decline of POA and sulfate concentrations. The plot of SOA vertical distribution also demonstrates that the majority of the SOA decrease takes place in the Northern Hemisphere.

The decreased aerosol acidity level in the future is predicted to amplify the reduction of SOA caused by the decreased sulfate surface area. However, this amplification effect is very limited (Table 1). The decrease in global SOA burden changes from −2% to −5% when considering the influence of aerosol acidity. Regionally, the surface IEPOX SOA concentration averaged over the North America is decreased by 31% when the aerosol acidity effect is excluded (CL2000_EM2100 - CL2000_EM2000) and by 34% when the aerosol acidity effect is included (CL2000_EM2100_pH - CL2000_EM2000_pH).

4.2. Effect of Climate Change

Global isoprene emission is predicted to increase by 18% in year 2100 (CL2100_EM2000-CL2000_EM2000) mainly due to the increased surface temperature and CO_2 concentration (Table 1). CAM5 projects an increase of 4.02°C in global averaged surface air temperature under the RCP 8.5 scenario, which causes the temperature activity factor (a factor that accounts for the emission change due to the temperature change) to increase by 99% globally. The increase in CO_2 concentration, on the other hand, decreases the global mean isoprene emission activity factor associated with CO_2 inhibition by 43%. The isoprene emissions activity factors associated with LAI and light change slightly, within 3% of year 2000 values. Therefore, the major drivers for isoprene emission change are the CO_2 inhibition effect and surface temperature increase effect. These two effects cancel each other to some extent, resulting in an 18% increase in isoprene emissions. This increase is compared to a decrease of 8% in isoprene emission predicted from Community Climate System Model version 3 (CCSM3) (CAM3/CLM3.5) projections [*Heald et al.*, 2009]. The different sign of change is attributed to different climate sensitivity and to different short-term isoprene response to CO_2. The equilibrium climate sensitivity in CCSM3 is 2.7°C [*Meehl et al.*, 2006], while the value is 4.1°C in CESM1 (CAM5) [*Meehl et al.*, 2013]. In the CO_2 suppression parameterization of *Wilkinson et al.* [2009] used in both CCSM3 and CESM1, the sensitivity of the isoprene emission rate to the short-term exposure of CO_2 decreases with increasing CO_2 concentrations. The suppression of isoprene by elevated CO_2 concentrations is thus weaker for the 943 ppmv CO_2 predicted using RCP 8.5 than that for the 717 ppmv predicted under the Special Report on Emissions Scenarios A1B scenario used in *Heald et al.* [2009].

The global SOA burden is estimated to increase by 25% as a result of climate change using present-day anthropogenic emissions (CL2100_EM2000-CL2000_EM2000). Climate change influences SOA concentrations in several ways. First, the increase in the BVOC emission rate enhances SOA concentrations because biogenic SOA comprises a large fraction of total SOA. The spatial distribution of the change in surface SOA concentration is generally in line with the spatial pattern of change in isoprene emissions (Figures S3c and S4a), with the largest increase over Europe, Central Africa, and South America, as well as their outflow regions. Second,

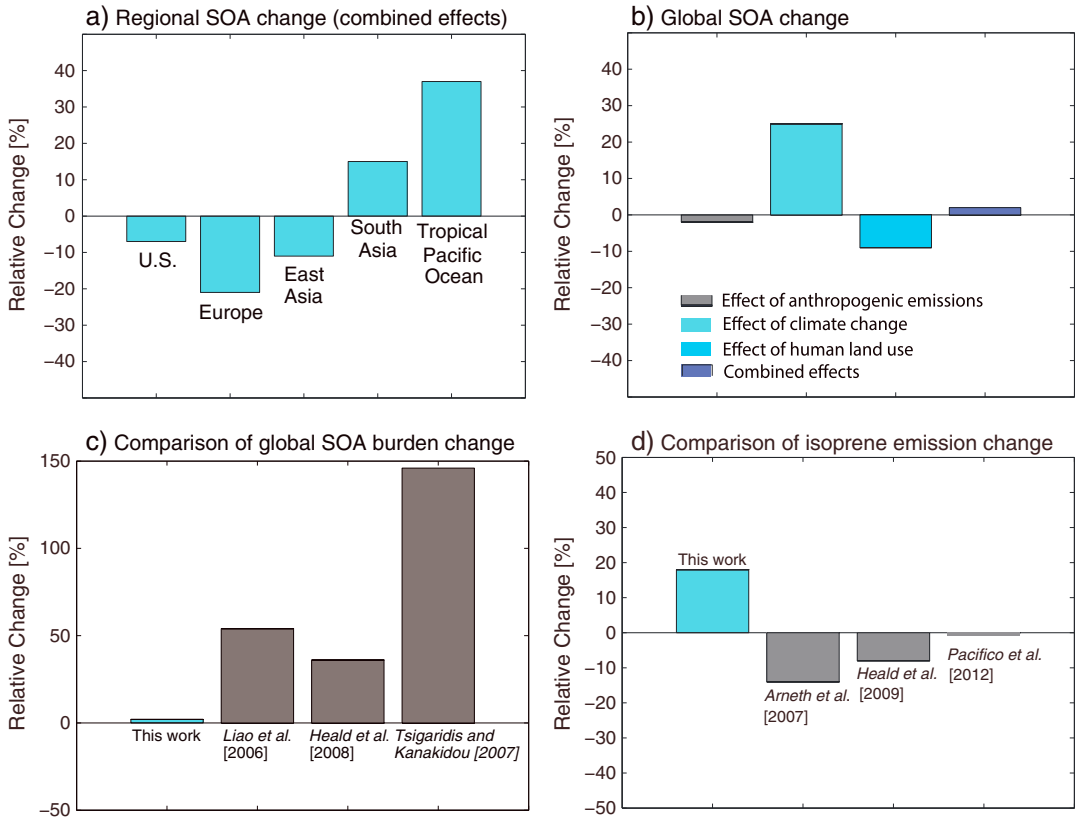

Figure 2. (a) Projected year 2000 to year 2100 relative change ((year 2100–year 2000)/year 2000) in regional mean SOA burden over the United States, Europe, East Asia, South Asia, and the Tropical Pacific Ocean, due to the combined effects of changes to anthropogenic emissions, climate, and anthropogenic land use change. (b) Projected relative change in global SOA burden in response to changes in anthropogenic emissions, climate, anthropogenic land use change, and their combined effects. Comparison with previous studies of (c) global SOA change and (d) isoprene emission change.

the change in precipitation rates affects the aerosol lifetime and thus SOA concentrations. The CESM predicts more precipitation in tropical regions and less precipitation in subtropical regions for RCP 8.5 in year 2100 compared to year 2000 [*Meehl et al*., 2013]. The larger precipitation rate can explain the lower SOA concentrations over the tropical Africa outflow region, and the smaller summer precipitation over the Pacific Ocean near Peru can contribute to the SOA increase there (Figure S3c). On a global basis, the annual SOA lifetime increases from 7.0 days for year 2000 to 7.4 days for year 2100, amplifying the global SOA burden increase. Also, there are several other direct and indirect ways in which climate change can impact SOA concentrations. These include through enhancing water vapor, increasing lightning NO_x emissions, temperature-dependent chemical reaction rates, and changing gas-particle partitioning and cloud water content, but these mechanisms are generally expected to be small relative to the effects of climate change on biogenic emissions. For example, the decreased cloud water content decreases the global SOA production rate by about 1%, compared to an 18% increase due to the increase in isoprene emission rate.

4.3. Effect of Anthropogenic Land Use Change

Figure S3e shows the spatial distribution of the change in isoprene emissions in the year 2100 due to the human land use change under the RCP 8.5 scenario (CL2100_EM2100_LND-CL2100_EM2100). The increase in isoprene emissions over Europe and eastern China reflects afforestation in these regions in the year 2100, while the reduction in isoprene emissions over South America, sub-Saharan Africa, and India, reflects cropland expansion in the year 2100. Globally, the isoprene emission rate declines by 52 Tg/yr (11.8% of year 2000 isoprene emission rate). This is consistent with the 15% decrease of isoprene emissions reported by *Heald et al*. [2008], which studied the effect of the Intergovernmental Panel on Climate Change A2 scenario land use change. The change in human land use alone causes the global SOA burden to decrease by 14%

primarily as a consequence of the BVOC emission decrease. The spatial pattern of the SOA change (Figure S3e) generally reflects the change in isoprene emissions (Figure S4b), with the major change over South America and sub-Saharan Africa.

4.4. Combined Effect of Changes in Anthropogenic Emissions, Climate, and Anthropogenic Land Use

The combined changes of anthropogenic emission and climate result in a 1.23 Tg SOA burden for year 2100 (CL2100_EM2100), 16% higher than that in year 2000 (Table 1). Figure S3g shows the spatial distribution of this change in SOA concentrations. While SOA decreases in the Northern Hemisphere, increases occur in tropical regions and the Southern Hemisphere. However, when changes in land use and land cover are included, the year 2100 global SOA burden (CL2100_EM2100_LND) declines to 1.08 Tg, only 2% higher compared to year 2000 burden (Table 1). The weak change in global SOA burden between year 2000 and year 2100 is in contrast to the strong increase of 36% to over 100% estimated by previous studies [*Liao et al*., 2006; *Tsigaridis and Kanakidou*, 2007; *Heald et al*., 2008]. Despite the nearly constant global SOA burden from year 2000 to year 2100, regional SOA concentrations show large variations (Figure 2a). Regional mean SOA concentration decreases by 7% over United States, 21% over Europe, and 11% over East Asia, but it increases by 15% over South Asia and 37% over tropical Pacific Ocean (−10° to 10°N, 90° to 180°W).

5. Conclusions and Discussion

We examined the sensitivity of SOA concentrations to changes in emission, climate, and anthropogenic land use and land cover at the end of 21st century following the RCP 8.5 scenario. We find that the global SOA burden is most sensitive to climate change, followed by anthropogenic land use and land cover change (Figure 2b). Climate change increases isoprene emissions by 18% due to rising temperatures, even though the CO_2 inhibition effect offsets this increase. In addition to isoprene emission increases, climate change alone elevates global SOA by 25%. Anthropogenic land use and land cover change alone reduces global SOA by 14%, and anthropogenic emission change alone increases global SOA by 2%. Integrating these three effects together results in only a small change in the global SOA burden. Previously neglected heterogeneous reactions in aerosol water and on aerosol surface play an important role in the SOA change. The control of sulfur emissions in the future reduces SOA formation, leading to lower SOA concentrations over the Northern Hemisphere (Figure 1c).

However, there are still substantial uncertainties associated with the projection of future SOA, mainly resulting from uncertainty in the CO_2 inhibition effect on BVOC emissions, in changes to natural vegetation, and in SOA sources and sinks. Because of incomplete knowledge of the CO_2 suppression effect on isoprene emissions [*Sharkey and Monson*, 2014], estimates of future isoprene emissions can differ depending on the exact form of CO_2-isoprene interaction parameterization. Utilization of the parameterization by [*Possell and Hewitt* 2011], for example, is expected to reduce the isoprene emission more than that in this study, which used the *Wilkinson et al*. [2009] parameterization. However, many observations have suggested that this CO_2 suppression effect is reduced at increased leaf temperatures [e.g., *Sun et al*., 2013]. Natural vegetation change in response to climate change is another source of uncertainty for future isoprene emissions. Potential natural vegetation changes predicted by dynamic vegetation models can differ substantially among different climatic predictions [*Yu et al*., 2014] and different vegetation models [*Sitch et al*., 2008; *Carslaw et al*., 2010] (i.e., a 25% to 260% increase in isoprene emissions). Given this large uncertainty, we did not include the effects of changes to natural vegetation. However, we acknowledge that this effect might play an important role in the change in isoprene emissions. The third uncertainty is related to SOA formation mechanisms. The sources, sinks, and chemistry of SOA are uncertain [*Lin et al*., 2012, 2014; *Tsigaridis et al*., 2014] due to the huge number of different atmospheric organic molecules and the complex physical and chemical processes controlling the conversion of gas phase organics to aerosol [*Hallquist et al*., 2009]. Our SOA model includes more processes than most of other current existing models and is one of the most complex SOA models [*Tsigaridis et al*., 2014]. Such complexity is needed to reflect the complexity and the dynamics of real SOA system and to better quantify the response of SOA to climate change and human activities [*Tsigaridis et al*., 2014].

The following three key findings in this paper have not been reported previously.1. We find only a small change in the global SOA burden in the future. This is in contrast to the strong increase of 36% to over 100% estimated in previous studies [*Liao et al*., 2006; *Tsigaridis and Kanakidou*, 2007; *Heald et al*., 2008]

(Figure 2c).2. We predict an increase of 18% in isoprene emissions due to the effect of climate change, which is opposite to previous findings of small or negative change [*Pacifico et al*., 2012; *Arneth et al*., 2007; *Young et al*., 2009; *Heald et al*., 2009] (Figure 2d).3. Decreases in future sulfur emissions as well as anthropogenic land use change lead to reductions in SOA concentrations, which counteract the effect of climate change in increasing isoprene emissions, leading to lower SOA concentrations over the Northern Hemisphere. These results call into question the projected increases in SOA by previous studies.

One limitation of this work is that the current model underestimates observed SOA in the Northern Hemisphere, which adds uncertainty to our projection of future SOA. Our projections are subject to this limitation as well as to limitations due to uncertainties in SOA formation and physics. These uncertainties could lead to changes in projections as new knowledge is developed. For example, a recent paper details some of the mechanisms leading to SOA formation from α-pinene [*Zhang et al*., 2015]. Implementation of the suggestions made there may lead to changes in our predicted future SOA.

Acknowledgments
This work was supported by Partnerships for Innovation in Sustainable Energy Technologies (PISET) program, Energy Institute, University of Michigan, Ann Arbor, MI, USA, and NASA grant NNX15AE34G to the University of Michigan. We thank Guiling Wang (University of Connecticut), Mark Flanner (University of Michigan), Chaoyi Jiao (University of Michigan), Justin Perket (University of Michigan), Bing Pu (University of Texas at Austin), Mingjie Shi (JPL), Colette Heald (MIT), and Louisa Emmons (NCAR) for their helpful discussions. We would like to acknowledge high-performance computing support from Yellowstone (ark:/85065/d7wd3xhc) provided by NCAR's Computational and Information Systems Laboratory, sponsored by the National Science Foundation. Model results can be accessed upon request to the corresponding author.

References

Arneth, A., et al. (2007), Process-based estimates of terrestrial ecosystem isoprene emissions: Incorporating the effects of a direct CO_2-isoprene interaction, *Atmos. Chem. Phys.*, *7*, 31–53.

Carlton, A. G., R. W. Pinder, P. V. Bhave, and G. A. Pouliot (2010), To what extent can biogenic SOA be controlled?, *Environ. Sci. Technol.*, *44*, 3376–3380, doi:10.1021/es903506b.

Carslaw, K. S., O. Boucher, D. V. Spracklen, G. W. Mann, J. G. L. Rae, S. Woodward, and M. Kulmala (2010), A review of natural aerosol interactions and feedbacks within the Earth system, *Atmos. Chem. Phys.*, *10*(4), 1701–1737, doi:10.5194/acp-10-1701-2010.

Eddingsaas, N. C., D. G. VanderVelde, and P. O. Wennberg (2010), Kinetics and products of the acid-catalyzed ring-opening of atmospherically relevant butyl epoxy alcohols, *J. Phys. Chem. A*, *114*(31), 8106–8113.

Ervens, B., B. J. Turpin, and R. J. Weber (2011), Secondary organic aerosol formation in cloud droplets and aqueous particles (aqSOA): A review of laboratory, field and model studies, *Atmos. Chem. Phys.*, *11*(21), 11,069–11,102, doi:10.5194/acp-11-11069-2011.

Gaston, C. J., T. P. Riedel, Z. F. Zhang, A. Gold, J. D. Surratt, and J. A. Thornton (2014), Reactive uptake of an isoprene-derived epoxydiol to submicron aerosol particles, *Environ. Sci. Technol.*, *48*(19), 11,178–11,186.

Guenther, A., T. Karl, P. Harley, C. Wiedinmyer, P. I. Palmer, and C. Geron (2006), Estimates of global terrestrial isoprene emissions using MEGAN (Model of Emissions of Gases and Aerosols from Nature), *Atmos. Chem. Phys.*, *6*, 3181–3210.

Guenther, A. B., X. Jiang, C. L. Heald, T. Sakulyanontvittaya, T. Duhl, L. K. Emmons, and X. Wang (2012), The model of emissions of gases and aerosols from nature version 2.1 (MEGAN2.1): An extended and updated framework for modeling biogenic emissions, *Geosci. Model Dev.*, *5*(6), 1471–1492, doi:10.5194/gmd-5-1471-2012.

Hallquist, M., et al. (2009), The formation, properties and impact of secondary organic aerosol: Current and emerging issues, *Atmos. Chem. Phys.*, *9*(14), 5155–5236.

Heald, C. L., et al. (2008), Predicted change in global secondary organic aerosol concentrations in response to future climate, emissions, and land use change, *J. Geophys. Res.*, *113*, D05211, doi:10.1029/2007JD009092.

Heald, C. L., M. J. Wilkinson, and R. K. Monson (2009), Response of isoprene emission to ambient CO_2 changes and implications for global budgets, *Global Change Biol.*, *15*(5), 1127–1140, doi:10.1111/J.1365-2486.2008.01802.X.

Hoyle, C. R., G. Myhre, T. K. Berntsen, and I. S. A. Isaksen (2009), Anthropogenic influence on SOA and the resulting radiative forcing, *Atmos. Chem. Phys.*, *9*, 2715–2728, doi:10.5194/acp-9-2715-2009.

Hu, W. W., et al. (2015), Characterization of a real-time tracer for isoprene epoxydiols-derived secondary organic aerosol (IEPOX-SOA) from aerosol mass spectrometer measurements, *Atmos. Chem. Phys. Discuss.*, *15*(8), 11,223–11,276, doi:10.5194/acpd-15-11223-2015.

Intergovernmental Panel on Climate Change (IPCC) (2013), *Climate Change 2013: The Physical Science Basis. Contribution of Working Group I to the Fifth Assessment Report of the Intergovernmental Panel on Climate Change*, edited by T. F. Stocker et al., 1535 pp., Cambridge Univ. Press, Cambridge, U. K.

Ito, A., S. Sillman, and J. E. Penner (2007), Effects of additional nonmethane volatile organic compounds, organic nitrates, and direct emissions of oxygenated organic species on global tropospheric chemistry, *J. Geophys. Res.*, *112*, D06309, doi:10.1029/2005JD006556.

Jimenez, J. L., et al. (2009), Evolution of organic aerosols in the atmosphere, *Science*, *326*(5959), 1525–1529, doi:10.1126/science.1180353.

Kulmala, M., et al. (2004), A new feedback mechanism linking forests, aerosols, and climate, *Atmos. Chem. Phys.*, *4*(2), 557–562, doi:10.5194/acp-4-557-2004.

Lamarque, J. F., L. K. Emmons, and P. G. Hess (2012), CAM-Chem: Description and evaluation of interactive atmospheric chemistry in the Community Earth System Model, *Geosci. Model Dev.*, *5*, 369–411, doi:10.5194/gmd-5-369-2012.

Lane, T. E., N. M. Donahue, and S. N. Pandis (2008), Effect of NO_x on secondary organic aerosol concentrations, *Environ. Sci. Technol.*, *42*(16), 6022–6027.

Lathiere, J., D. A. Hauglustaine, N. De Noblet-Ducoudré, G. Krinner, and G. A. Folberth (2005), Past and future changes in biogenic volatile organic compound emissions simulated with a global dynamic vegetation model, *Geophys. Res. Lett.*, *32*, L20818, doi:10.1029/2005GL024164.

Lawrence, D. M., et al. (2011), Parameterization improvements and functional and structural advances in version 4 of the Community Land Model, *J. Adv. Model. Earth Syst.*, *3*, M03001, doi:10.1029/2011MS000045.

Lawrence, P. J., et al. (2012), Simulating the biogeochemical and biogeophysical impacts of transient land cover change and wood harvest in the Community Climate System Model (CCSM4) from 1850 to 2100, *J. Clim.*, *25*(9), 3071–3095, doi:10.1175/JCLI-D-11-00256.1.

Liao, H., W. T. Chen, and J. H. Seinfeld (2006), Role of climate change in global predictions of future tropospheric ozone and aerosols, *J. Geophys. Res.*, *111*, D12304, doi:10.1029/2005JD006852.

Lin, G., J. E. Penner, S. Sillman, D. Taraborrelli, and J. Lelieveld (2012), Global modeling of SOA formation from dicarbonyls, epoxides, organic nitrates and peroxides, *Atmos. Chem. Phys.*, *12*(10), 4743–4774, doi:10.5194/acp-12-4743-2012.

Lin, G., S. Sillman, J. E. Penner, and A. Ito (2014), Global modeling of SOA: The use of different mechanisms for aqueous-phase formation, *Atmos. Chem. Phys.*, *14*(11), 5451–5475, doi:10.5194/acp-14-5451-2014.

Liu, H., D. J. Jacob, I. Bey, and R. M. Yantosca (2001), Constraints from ^{210}Pb and ^{7}Be on wet deposition and transport in a global three-dimensional chemical tracer model driven by assimilated meteorological fields, *J. Geophys. Res.*, *106*(D11), 12,109–12,128, doi:10.1029/2000JD900839.

Mari, C., D. J. Jacob, and P. Bechtold (2000), Transport and scavenging of soluble gases in a deep convective cloud, *J. Geophys. Res.*, *105*, 22,255–22,267, doi:10.1029/2000JD900211.

Meehl, G. A., W. M. Washington, B. D. Santer, W. D. Collins, J. M. Arblaster, A. Hu, D. M. Lawrence, H. Teng, L. E. Buja, and W. G. Strand (2006), Climate change projections for the twenty-first century and climate change commitment in the CCSM3, *J. Clim.*, *19*(11), 2597–2616.

Meehl, G. A., W. M. Washington, J. M. Arblaster, A. Hu, H. Teng, J. E. Kay, A. Gettelman, D. M. Lawrence, B. M. Sanderson, and W. G. Strand (2013), Climate change projections in CESM1(CAM5) compared to CCSM4, *J. Clim.*, *26*(17), 6287–6308, doi:10.1175/JCLI-D-12-00572.1.

Nguyen, T. K. V., S. L. Capps, and A. G. Carlton (2015), Decreasing aerosol water is consistent with OC trends in the southeast U.S., *Environ. Sci. Technol.*, doi:10.1021/acs.est.5b00828.

Pacifico, F., G. A. Folberth, C. D. Jones, S. P. Harrison, and W. J. Collins (2012), Sensitivity of biogenic isoprene emissions to past, present, and future environmental conditions and implications for atmospheric chemistry, *J. Geophys. Res.*, *117*, D22302, doi:10.1029/2012JD018276.

Pankow, J. F. (1994), An absorption model of gas/particle partitioning of organic compounds in the atmosphere, *Atmos. Environ.*, *28*(2), 185–188, doi:10.1016/1352-2310(94)90093-0.

Perket, J., M. G. Flanner, and J. E. Kay (2014), Diagnosing shortwave cryosphere radiative effect and its 21st century evolution in CESM, *J. Geophys. Res. Atmos.*, *119*, 1356–1362, doi:10.1002/2013JD021139.

Piletic, I. R., E. O. Edney, and L. J. Bartolotti (2013), A computational study of acid catalyzed aerosol reactions of atmospherically relevant epoxides, *Phys. Chem. Chem. Phys.*, *15*(41), 18,065–18,076.

Possell, M., and C. N. Hewitt (2011), Isoprene emissions from plants are mediated by atmospheric CO_2 concentrations, *Global Change Biol.*, *17*(4), 1595–1610.

Pye, H. O. T., et al. (2013), Epoxide pathways improve model predictions of isoprene markers and reveal key role of acidity in aerosol formation, *Environ. Sci. Technol.*, *47*(19), 11,056–11,064.

Riedel, T. P., Y.-H. Lin, S. H. Budisulistiorini, C. J. Gaston, J. A. Thornton, Z. Zhang, W. Vizuete, A. Gold, and J. D. Surratt (2015), Heterogeneous reactions of isoprene-derived epoxides: Reaction probabilities and molar secondary organic aerosol yield estimates, *Environ. Sci. Technol. Lett.*, *2*(2), 38–42, doi:10.1021/ez500406f.

Seinfeld, J. H., and S. N. Pandis (1998), *Atmospheric Chemistry and Physics: From Air Pollution to Climate Change*, John Wiley, New York.

Sharkey, T. D., and R. K. Monson (2014), The future of isoprene emission from leaves, canopies and landscapes, *Plant Cell Environ.*, *37*(8), 1727–1740, doi:10.1111/pce.12289.

Sitch, S., et al. (2008), Evaluation of the terrestrial carbon cycle, future plant geography and climate-carbon cycle feedbacks using five Dynamic Global Vegetation Models (DGVMs), *Global Change Biol.*, *14*(9), 2015–2039, doi:10.1111/j.1365-2486.2008.01626.x.

Sun, Z., K. Huve, V. Vislap, and Ü. Niinemets (2013), Elevated [CO_2] magnifies isoprene emissions under heat and improves thermal resistance in hybrid aspen, *J. Exp. Bot.*, *64*(18), 5509–5523, doi:10.1093/jxb/ert318.

Tai, A. P. K., L. J. Mickley, C. L. Heald, and S. Wu (2013), Effect of CO_2 inhibition on biogenic isoprene emission: Implications for air quality under 2000 to 2050 changes in climate, vegetation, and land use, *Geophys. Res. Lett.*, *40*, 3479–3483, doi:10.1002/grl.50650.

Tsigaridis, K., and M. Kanakidou (2007), Secondary organic aerosol importance in the future atmosphere, *Atmos. Environ.*, *41*(22), 4682–4692, doi:10.1016/j.atmosenv.2007.03.045.

Tsigaridis, K., et al. (2014), The AeroCom evaluation and intercomparison of organic aerosol in global models, *Atmos. Chem. Phys.*, *14*(19), 10,845–10,895, doi:10.5194/acp-14-10845-2014.

Unger, N. (2013), Isoprene emission variability through the twentieth century, *J. Geophys. Res. Atmos.*, *118*, 13,606–13,613, doi:10.1002/2013JD020978.

Van Vuuren, D. P., J. Edmonds, M. Kainuma, K. Riahi, A. Thomson, K. Hibbard, G. C. Hurtt, T. Kram, V. Krey, and J.-F. Lamarque (2011), The representative concentration pathways: An overview, *Clim. Change*, *109*, 5–31.

Wesely, M. L. (1989), Parameterization of surface resistances to gaseous dry deposition in regional-scale numerical models, *Atmos. Environ.*, *23*, 1293–1304.

Wilkinson, M. J., R. K. Monson, N. Trahan, S. Lee, E. Brown, R. B. Jackson, H. W. Polley, P. A. Fay, and R. Fall (2009), Leaf isoprene emission rate as a function of atmospheric CO_2 concentration, *Global Change Biol.*, *15*(5), 1189–1200, doi:10.1111/j.1365-2486.2008.01803.x.

Xu, L., et al. (2015), Effects of anthropogenic emissions on aerosol formation from isoprene and monoterpenes in the south-eastern United States, *Proc. Natl. Acad. Sci. U.S.A.*, *112*, 37–42, doi:10.1073/pnas.1417609112.

Young, P. J., A. Arneth, G. Schurgers, G. Zeng, and J. A. Pyle (2009), The CO_2 inhibition of terrestrial isoprene emission significantly affects future ozone projections, *Atmos. Chem. Phys.*, *9*(8), 2793–2803, doi:10.5194/acp-9-2793-2009.

Yu, M., G. Wang, D. Parr, and K. F. Ahmed (2014), Future changes of the terrestrial ecosystem based on a dynamic vegetation model driven with RCP8.5 climate projections from 19 GCMs, *Clim. Change*, *127*(2), 257–271, doi:10.1007/s10584-014-1249-2.

Zhang, X., R. C. McVay, D. D. Huang, N. F. Dalleska, B. Aumont, R. C. Flagan, and J. H. Seinfeld (2015), Formation and evolution of molecular products in α-pinene secondary organic aerosol, *Proc. Natl. Acad. Sci. U.S.A.*, *112*, 14,168–14,173, doi:10.1073/pnas.1517742112.

Zhou, C., and J. E. Penner (2014), Aircraft soot indirect effect on large-scale cirrus clouds: Is the indirect forcing by aircraft soot positive or negative?, *J. Geophys. Res. Atmos.*, *119*, 11,303–11,320, doi:10.1002/2014JD021914.